

PRELIMINARY OBSERVATIONS FROM THE AURORAL AND IONOSPHERIC REMOTE SENSING IMAGER

The Auroral and Ionospheric Remote Sensing Experiment on board the Polar BEAR satellite uses a four-color imager covering selected wavelengths in the visible/near-UV and vacuum ultraviolet (110.0- to 180.0-nm ranges). This device is capable of imaging global auroral display and the distribution of atmospheric emissions in both dark and sunlit regions. In addition to providing images, it can also operate in either spectrometric or photometric modes. This article describes the techniques employed and gives preliminary observations from the experiment.

INTRODUCTION

Modern auroral science has progressed in steps from the pioneering years of 1900 to 1930. The first auroral "imaging" consisted of sketches made during the first Polar Year (1882–1883). Photography was introduced into auroral science at the beginning of this century and was used in classification and height determination by Störmer.¹ Between 1930 and 1955, great advances were made in spectroscopic study of the aurora; prominent auroral emissions, such as those at 486.1 nm from the hydrogen atom, 557.7 nm from atomic oxygen, and 391.4 nm from N_2^+ , were identified. About 1955, S. Chapman and C. T. Elvey recognized a serious need for global auroral imaging; recognition of that need led to the simultaneous operation of more than 100 ground-based "all-sky" cameras in the northern and southern polar regions during the International Geophysical Year (1957–1958). The global auroral imaging acquired through this first effort showed that the auroras were located along a belt called the auroral oval, rather than in the classical auroral zone distributed along the constant geomagnetic circles. It further brought forth the concept of the auroral substorm, which described the basic cycle of activity that the auroras undergo globally during intense magnetic storm disturbances.² This concept assumed added importance when it was found that other polar and magnetospheric disturbance phenomena occur in harmony with the auroral substorm. The term "magnetospheric substorm" was then evolved to describe the basic cycle of magnetospheric disturbances, and the auroral substorm is now regarded as one of the manifestations of the magnetospheric substorm.³

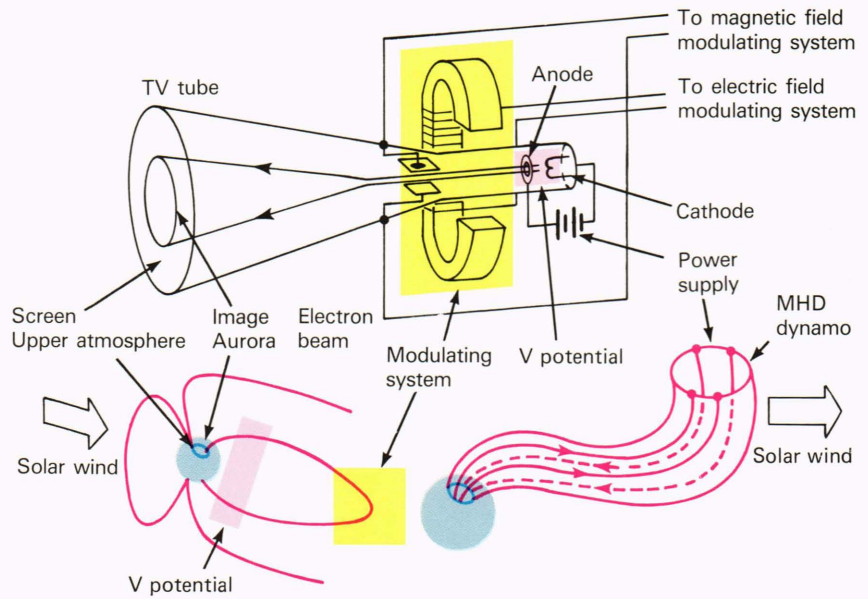
To illustrate the importance of auroral images in magnetospheric studies, it is useful to consider the crude analogy between a cathode ray (or TV) tube and the magnetosphere (Fig. 1). The screen of the tube corresponds to the polar upper atmosphere, and an image on the screen corresponds to the aurora. Various modulating devices in the tube cause the electron beam and the multicolor image to form and to move on the screen. Similarly, auroral activity indicates complex disturbances in the elec-

tric and magnetic fields in the magnetosphere. Magnetospheric physicists have been seeking answers to these key questions: (a) How is the magnetosphere powered (the solar wind–magnetosphere interactions)? (b) What is the mechanism analogous to the electron gun and beam (the acceleration mechanism of auroral electrons)? (c) How is the electron beam modulated (the magnetospheric substorm)? The importance of auroral imaging in addressing these questions is clear, especially since the auroral display is the only visible feature of the solar wind–magnetosphere interaction.

Auroral imaging made quantum progress from 1971 to 1973 as a result of the successful operation of imaging devices aboard the ISIS-2 and DMSP satellites; one picture of global auroral distribution was obtained in each orbit. DMSP images dramatically confirmed results of the early ground-based all-sky photographic studies of the auroral substorm.

After 1960, auroral spectroscopy advanced by observing the auroral vacuum ultraviolet (VUV) emissions. During the past 25 years, study of these emissions has provided a wealth of new information about the physical and chemical effects of energetic particle precipitation and about the relationship between the observed emissions and the energy spectrum of the incident particles. As technology progressed during the 25 years, spectral resolution was significantly improved; extension of spectroscopic measurements to wavelengths below 120.0 nm became feasible.⁴ From the very first rocket flight for auroral VUV studies,⁵ the principal features of the auroral VUV emission spectrum were identified to be electron-excited transitions of the principal atmospheric species, N_2 and O. Lines of atomic nitrogen were subsequently identified. Below 200.0 nm, the N_2 emissions are all in the Lyman–Birge–Hopfield (LBH) system, the strongest bands of which occur between 132.5 and 150.0 nm; the atomic oxygen transitions are the (3S – 3P) resonance triplet at 130.4 nm and the (5S – 3P) doublet at 135.6 nm. The Lyman α ($L\alpha$) line of atomic hydrogen at 121.6 nm is always present, ow-

Figure 1—Schematic diagram illustrating the analogy between the television tube and the magnetosphere. Auroras in the polar upper atmosphere are produced by electron-beam bombardment, much as images are produced on a TV screen. The electromagnetic state of the magnetosphere modulates the electron beams in a manner similar to modulation by the electric plate and electromagnet within the TV tube. Some magnetospheric physicists believe that the power for the auroral phenomenon is derived from the MHD dynamo action of solar wind blowing across the “open” geomagnetic field lines, and that the acceleration mechanism for the electron beams is the V potential along geomagnetic field lines.



ing to resonance scattering of sunlight by the extended hydrogen geocorona, but enhancements of $L\alpha$, indicating proton precipitation, have been observed.⁶

Identification of the strong emission features made it possible to consider using VUV photometers or spectrometers on orbiting nadir-looking platforms to study the global morphology of aurora, especially on the sunlit hemisphere, since the albedo of the lower atmosphere at these wavelengths is effectively zero. Examples of such efforts were the OGO-4 polar orbiting satellite⁶ and the Air Force Space Test Program (STP) S3-4 and P78-1 satellites,^{7,8} which provided the latitudinal profiles of certain VUV emissions without a global imaging capability. Studies of auroral emissions features at wavelengths below 120.0 nm are just beginning. The spectral region between 120.0 and 170.0 nm, on the other hand, is now well understood in terms of precipitating-particle excitation of the principal atmospheric constituents; it is therefore well suited for the auroral imaging mission.

The Auroral Ionospheric Mapper (AIM) experiment on the HILAT satellite demonstrated that auroral displays over the sunlit polar region can be imaged by monitoring the VUV emissions;⁹ the present experiment on the Polar BEAR satellite is a refined technique of auroral and atmospheric remote sensing.

SCIENTIFIC OBJECTIVES

Magnetospheric Studies

The configuration of the magnetosphere is controlled by the solar wind, the interplanetary magnetic field (IMF), and the distribution of plasmas and electric currents in the magnetosphere. The combined effects of these influences divide the magnetosphere into two basic regions, the so-called “closed-field” region and the “open-field” region. The auroral oval delineates approximately the boundary of the two regions at the ionospheric level. Changes of this boundary, and thus of the

auroral oval, indicate major internal changes in the structure of the magnetosphere, resulting from changes of the solar wind and the IMF. Thus, the size of the auroral oval provides a measure of the magnetic flux in the magnetotail and of magnetic energy in the magnetotail (since the radius of the magnetotail does not change significantly with geomagnetic conditions). Imaging of global auroral activity and simultaneous observation of the solar wind, the IMF, and magnetosphere dynamics can, together with data obtained from ground-based instrumentation, provide more quantitative measures of the interaction between the solar wind, the IMF, and the magnetosphere.

Atmospheric and Ionospheric Studies

In addition to the solar-terrestrial coupling studies, the quantitative measurements of atmospheric emissions enable us to investigate energy deposition and to conduct aeronomical studies. One of the important functions of the imager is to perform global remote sensing of the energy coupling between the magnetosphere and the terrestrial atmosphere that is produced by auroral particle precipitation. This precipitation causes ionization in the ionosphere, mostly in the auroral oval and the polar cap. Of all the energy deposited by the bombardment of typical auroral particles, only a few percent is radiated as optical emissions.

The intensity of this optical radiation provides, however, a very effective means of monitoring the global energy deposition. A conventional technique is to monitor intensity of the N_2^+ 1 negative bands at 391.4 or 427.8 nm. The conversion ratio from intensity of the 391.4-nm emission to energy flux is about 600 R (rayleighs)/erg $cm^{-2}s^{-1}$. The emission of the N_2 2nd positive system can also be used, and the (0,0) band of this system is at 337.1 nm. Both the 391.4- and 337.1-nm emissions are included as narrow-band filters in the visible part of our imager. The mean energy of the particle precipitation can

also be deduced from optical emissions. The underlying principle is that precipitating electrons of different energies are stopped at different heights, where they excite atmospheric species according to their abundances at that altitude. If emission intensities are measured at two wavelengths, a fit to a two-parameter differential energy distribution can be made. The intensity ratio of 630.0/391.4 nm is commonly used to infer the mean energy of auroral electron precipitation.

APPROACH TO INSTRUMENTATION

The experiment designed to demonstrate the global imaging technique using auroral and ionospheric remote sensing (AIRS) is on board the Polar BEAR satellite. The imagery is produced by the combination of the cross-track horizon-to-horizon line scan and the forward motion of a three-axis-stabilized spacecraft. The detector system consists of a $\frac{1}{8}$ -m spectrometer with (a) two photomultiplier tubes covering the 115.0- to 190.0-nm wavelength range (spectral resolution of 3.0 nm) and (b) a near-UV/visible system of a four-position filter wheel coupled with two UV/visible photomultiplier tubes. Thus, four images are made simultaneously by AIRS, two in the VUV wavelengths and two in the near-UV/visible wavelengths. A detailed description of the AIRS instrument can be found in the article by Schenkel and Ogorzalek elsewhere in this issue. The advantages of the AIRS experiment are

1. Simultaneous 4-wavelength measurements from the same footprint area,
2. Narrow 3.0-nm VUV bandpath imaging not possible using interference filters,
3. Three alternative modes of operation—imaging, spectrometer, or photometer—by controlling the scan mirror and the spectrometer gridding motor.

The design approach is similar to that of the AIM experiment on board the HILAT satellite; the improvements here are the combination of the near-UV/visible detectors with the imaging system and the addition of another VUV detector in the spectrometer.

PRELIMINARY OBSERVATIONS

The Polar BEAR spacecraft was successfully launched on November 13, 1986, and the AIRS imager has been operational since November 22, 1986. The polar-region auroral display has been routinely recorded by high-latitude ground data receiving stations since December 3, 1986. In this section, observations from two passes are used to illustrate two types of global auroral display. They are shown merely as preliminary examples of successful AIRS observations and are not intended as a complete illustration of the various kinds of auroral activity.

During geomagnetically quiet periods, the auroral display is rather unspectacular, and its brightness is very weak in all wavelength bands (from VUV to visible). Figure 2 (~0500 UT, January 30, 1987) illustrates such a condition. It covers the global image of the major portions of the auroral oval at 135.6 ± 15 nm of OI and

N_2 LBH emissions. The image is presented in geomagnetic latitude and local time coordinates; the landmass below the 80° geographic latitude circle is shown. The noon and midnight meridian almost bisects this diagram vertically; the dawn sector is on the right and the dusk sector is on the left (i.e., the figure gives a bird's-eye view of the auroral display over the northern polar region from 1000 km altitude). A weak diffuse glow forms the auroral oval, but the noon part of the oval (0900 to 1500 local time sector) was not recorded during this station pass. The intensity of the emissions at 135.6 ± 15 nm is presented by false color, as indicated in a color bar on the right side of the figure. White and red indicate greater brightness; black and blue indicate very weak intensity. The morning part of the oval is slightly brighter, about 100 to 400 R, whereas the dusk and midnight parts of the oval have intensities generally near 100 R or lower. The threshold of the detector at this wavelength is about 30 R. The simultaneous image at 159.6 ± 15 nm (not shown in this figure) also indicates a very weak emission (below 100 R at one or two counts level), and the auroral oval is barely discernible. Figure 3 (~0500 UT, January 30, 1987) is the corresponding image of the emission at 391.4 ± 5 nm, in the near-UV. Comparing Figures 2 and 3, the auroral oval for emissions at 391.4 nm can be identified, though it is not prominent. The emission brightness is about 1 kR (at 1 or 2 counts level and only slightly above the thermal noise background of the detector). The bright red and yellow

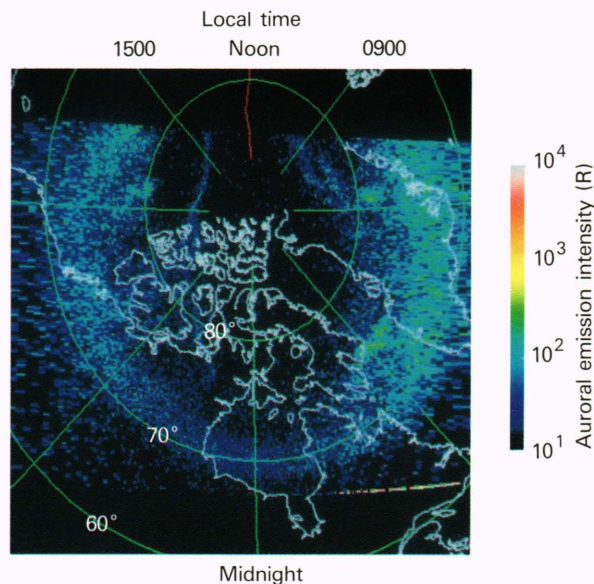


Figure 2—An example of the global auroral display during a geomagnetically quiet period ($\Sigma K_p = 7_0$; $K_p = 0_+$) on January 30, 1987, at 0507:17–0516:42, observed from Sondre Stromfjord station. It is a false-color presentation; the color bar at right indicates the intensity scale of the auroral emission at 135.6 ± 15 nm. The midday part of the auroral oval was not recorded. The auroral oval is oriented with the noon meridian toward the top and the midnight meridian toward the bottom. The dawn sector is on the right and the dusk sector is on the left. Note the faint diffused aurora, without significant discrete features, along the oval. The auroral emission at this wavelength band was below 400 R.

striation at the top of the image is associated with the glint of scattered sunlight after sunrise at the spacecraft's altitude during this ascending pass.

When geomagnetic activity increases, auroral activity also increases, and its display becomes more complicated. Figure 4 illustrates the moderately active auroral oval (~ 0440 UT, January 29, 1987). Discrete auroral features are clearly evident near the midnight part of the auroral oval. The intensities of emissions at 135.6 ± 15 nm along

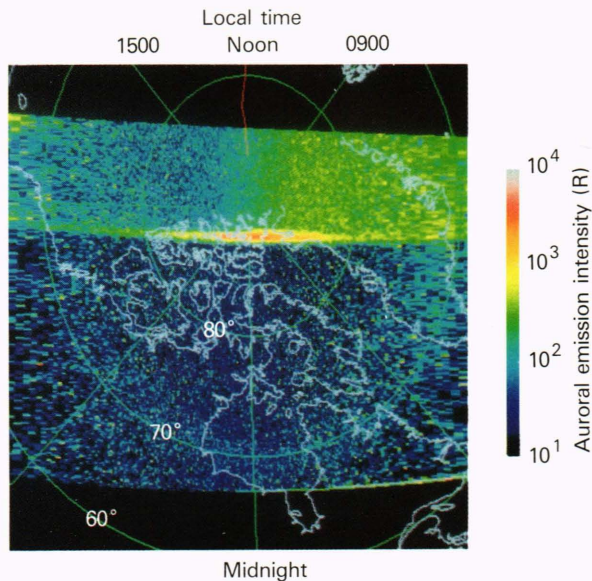


Figure 3—The near-UV (391.4 ± 5 nm) image corresponding to the observation in Fig. 2. The auroral oval is barely recognizable at this wavelength; emission intensity is about a few kilorayleighs and lower. The sudden enhanced brightness near the top of the picture is due to the satellite sunrise (i.e., some scattering of the sunlight by the satellite).

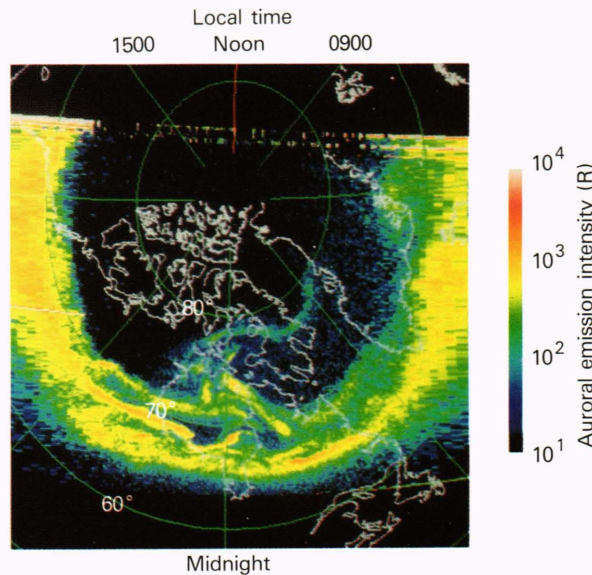


Figure 4—An example of the global auroral display during an active geomagnetic period on January 29, 1987, at 0436:19–0446:49, observed from Sondre Stromfjord station ($K_p = 3+$; $\Sigma K_p = 15$). Note the enhanced auroral brightness of a few kilorayleighs and active discrete auroral features in the midnight sector in this 135.8 ± 15 nm emission band.

the oval are generally about 1 kR, with discrete auroras of about 4 to 5 kR. These emissions are at least one order of magnitude brighter than during quiet times (compare Fig. 2). Figure 5 is the corresponding image of emissions at 159.6 ± 15 nm (mostly N_2 LBH emissions). The auroral features are similar to those in Fig. 4; because of the lesser sensitivity of the sensor at this wavelength, the image is more granular. The intensity is about a few hundred rayleighs. Figure 6 is the image from the same pass for emissions of wavelength 391.4 ± 5 nm. The oval background is of about 4 to 5 kR in-

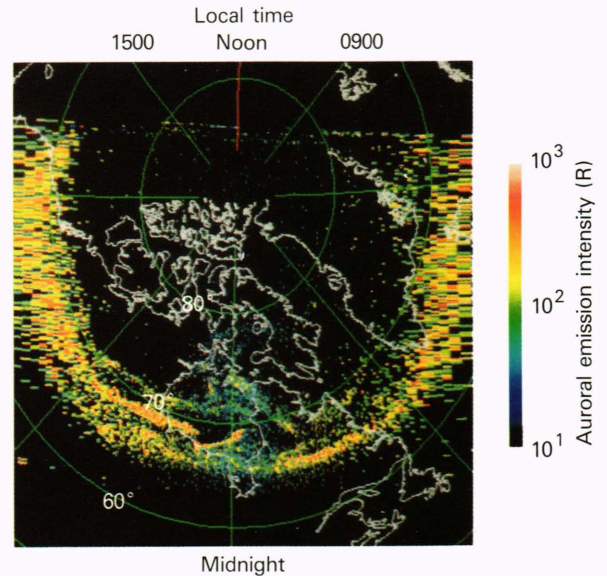


Figure 5—Simultaneous image corresponding to Fig. 4 but at a wavelength band of 159.7 ± 15 nm. Emission intensity up to about 600 R was observed. The auroral display imaged is very similar to the brightest part in Fig. 4.

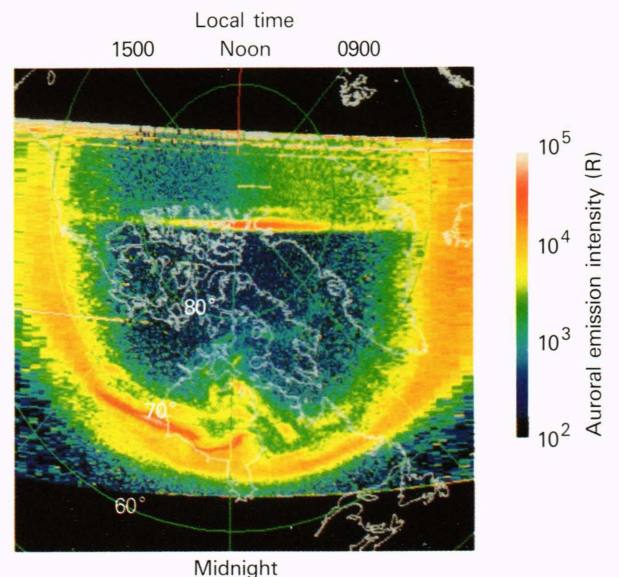


Figure 6—Simultaneous image corresponding to Fig. 4 but at near-UV wavelength (391.4 ± 5 nm). Note the very bright (up to about 60 kR) auroral display superposed on a nearly uniform auroral oval of about 20 kR.

tensity, with discrete auroras of up to about 100 kR; it is about two orders of magnitude brighter than the quiet-time auroral oval.

CONCLUSION

The AIRS experiment on board the Polar BEAR satellite is accomplishing its goal of globally imaging auroral displays and atmospheric emissions. Because of the satellite's higher altitude (~1000 km), most of the auroral oval can be imaged. Multicolor imaging can provide an additional dimension in global imaging capabilities for scientific research. Quantitative measurement of atmospheric and auroral emissions will enable us to investigate remote-sensing techniques of the atmospheric and ionosphere.

The purpose of this article has been merely to demonstrate the success of the instrument. Detailed scientific investigation using the AIRS data is in progress; results will be reported in the future.

REFERENCES

- ¹ C. Störmer, *The Polar Aurora*, Oxford University Press (1955).
- ² S.-I. Akasofu, "The Development of the Aurora Substorm," *Planet. Space Sci.* **12**, 273 (1964).
- ³ S.-I. Akasofu, *Polar and Magnetospheric Substorms*, D. Reidel Publ. Co., Dordrecht, Holland (1968).
- ⁴ H. Park, P. D. Feldman, and W. G. Fastie, "The Extreme Ultraviolet (750–1230 Å) Spectrum of an Aurora," *Geophys. Res. Lett.* **4**, 41 (1977).
- ⁵ W. G. Fastie, H. M. Crosswhite, and T. P. Markham, "Far Ultraviolet Auroral Spectra with a Rocket Ebert Spectrophotometer," *Ann. Geophys.* **17**, 109 (1981).
- ⁶ T. A. Chubb and G. T. Hicks, "Observations of the Aurora in the Far Ultraviolet from Ogo 4," *J. Geophys. Res.* **75**, 1290 (1970).
- ⁷ R. E. Huffman, F. J. Le Blanc, J. C. Larrabee, and D. E. Paulsen, "Satellite Vacuum Ultraviolet Airglow and Auroral Observations," *J. Geophys. Res.* **85**, 2701 (1980).
- ⁸ C.-I. Meng and S. Chakrabarti, "Extreme Ultraviolet Emissions for Monitoring Auroras in Dark and Daylight Hemispheres," *J. Geophys. Res.* **90**, 4261 (1985).
- ⁹ C.-I. Meng and R. E. Huffman, "Ultraviolet Imaging from Space of the Aurora Under Full Sunlight," *Geophys. Res. Lett.* **11**, 315 (1984).

THE AUTHORS



CHING I. MENG, was born in Sian, China, in 1940 and grew up in Taiwan. He came to the United States in 1963 to study polar geophysical phenomena based on data collected during the International Geophysical Year, such as the aurora and geomagnetic storms, at the Geophysical Institute of the University of Alaska. From 1969 to 1978, he was a research physicist at the Space Sciences Laboratory of the University of California at Berkeley specializing in the morphology of magnetospheric physics. Dr. Meng joined APL in 1978 and is involved in the investigation of solar-terrestrial interactions, plasma and field morphology of the magnetosphere, spacecraft charging, and the terrestrial atmosphere. He is also studying the global imaging of auroral display and atmospheric emissions.



ROBERT E. HUFFMAN was born in Breckenridge, Tex., in 1931 and earned a Ph.D. at the California Institute of Technology in 1958. He has been at the Air Force Geophysics Laboratory since 1958, where he is supervisor of the UV Surveillance Branch. He has published extensively in the fields of UV spectroscopy of atmospheric gases and in UV measurements of the earth's radiative environment. Dr. Huffman is principal investigator of the AIM UV-imaging sensor on the HILAT satellite and of the AIRS experiment on the Polar BEAR satellite. He was also principal investigator of the VUV backgrounds experiment on the S3-4 satellite and of the horizons UV program on a shuttle flight. He was program manager of Project Chaser and UV program manager of the Multispectral Measurements Program, programs that measured UV missile-exhaust plume characteristics.